Materials International
Open Access Journal (ISSN: 2668-5728)

Article
Volume 6, Issue 1, 2024, 4
https://doi.org/10.33263/Materials61.004

Synthesis of Ag NPs and their catalytic activity under ultrasonic irradiations

Pravin Chavan [1,*], Jagdish Thakur [1], Shivaji Jadhav [2], Dhanraj Kamble [3], Megha Rai [4], Rohini Shelke [5], Shoeb Sayyed [6,*], Dattatraya Pansare [7,*]

[1] Department of Chemistry, Doshi Vakil Arts College, and G.C.U.B. Science & Commerce College, Goregaon, Raigad 402103, MS, India
[2] Department of Chemistry, Tarai College of Arts and Science, Paithan, Aurangabad, MS, India
[3] Department of Chemistry, S. B.E.S. College of Science, Aurangabad 431001, Maharashtra, India
[4] Department of Chemistry, Dr. Rafiq Zakariya College for Woman, Aurangabad, MS, India
[5] Department of Chemistry, Radhabai Kale Mahila College Ahmednagar, 414001, MS, India
[6] Doshi Vakil Arts College, and G. C. U. B. Science & Commerce College, Goregaon, Raigad 402103, MS, India
[7] Department of Chemistry, Deogiri College, Station Road, Aurangabad 431 005, MS, India
* Correspondence: dattatraya.pansare7@gmail.com (D.P.), srsayyed786@gmail.com (S.S.);
Scopus Author ID 55623428200

Received: 2.04.2023; Accepted: 28.05.2023; Published: 19.02.2024

Abstract: The efficient green synthesis of Ag NPs was carried out via the reduction of aqueous silver nitrate using Antidesma Parvifolium leaf extract under ultrasonic irradiation. Prepared Ag NPs were monitored through various analytical spectroscopic techniques such as FTIR, UV-visible spectroscopy, XRD, FESEM, EDS, etc. Prepared nanomaterial showed excellent to good antimicrobial results. Prepared Ag NPs showed 21 nm spherical size. Newly designed Ag NPs were used as a catalyst for the synthesis of N-(7-R)-2-oxa-6-azabicyclo[3.2.0]heptan-6-yl)isonicotinamide derivatives (**4a-h**) utilizing a three-component one-pot reaction of Isoniazid with several aromatic aldehydes and dihydrofuran under ultrasonic irradiation is reported. Azetidine obtained moderate to significant yields (84-90%). The advantages of this synthetic protocol are that it is eco-friendly, highly efficient, inexpensive, easy to work with, and has significant yields.

Keywords: Ag NPs; One-pot three-component; cascade process; Isonicotinamide; ultrasonication.

1. Introduction

Nowadays, nanoparticles are a prominent field in the areas of engineering, physics, biology, and medicine, and others have recently included nanotechnology in their work [1]. Newer nanosized materials are being explored to afford significant and innumerable applications such as catalysis, cosmetics, food technology, nano-computers, space industry, bio-medical devices, nano-fertilizers, energy space, and sensors [2-5]. Till now, metallic nanoparticles (NPs) have been created from precious metals, including Platinum, Lead, Gold, and Silver, and used in items that come into touch with humans [6]. Therefore, as a result, developing an environmentally benign strategy for NPs synthesis rather than a hazardous route is critical [7]. Ag-NPs are among the metal NPs with a wide range of uses [8]. Ultrasonic irradiations, microwave and ultraviolet radiation, photochemical reduction, and Sono-electrochemical and photochemical procedures have all been used to create Ag-NPs. Among them, many routes are carried out using hazardous chemicals as reducing agents, potentially unsafe for living organisms and the environment [9, 10]. As we know, synthetic nanoparticles are toxic, and there is a demand to design biosynthetic procedures to create secure nanoparticles, including extraction-based NPs from plant *leaf*. Indeed, plant extracts contain several natural products that facilitate the formation and stabilization of NPs. On the other hand, the biosynthesis route using microorganisms, enzymes, and plant extracts is eco-friendly, fast, cost-effective, and optional to chemical and physical routes for the Ag-nanoparticle synthesis [11-16]. The plant extract technique is favorable because microorganisms are not required [17]. These NPs have a variety of unique features that make them interesting for use in numerous fields. Nowadays, researchers have reported several Ag NPs using various plant, seed, and fruit extract like *Withania somnifera*, [18] *Calendula officinalis*, [19-20] *Averrhoa bilimbi* [21] *Melia azedarach L.*,[22] *Silybum marianum*,[23], *Ulva flexuosa*, [24] *Nervalia zeylanica*,[25] *Beutia digitata* [26], *Caralluma fimbriata* [27], *Beutia monosperma* [28], *Ziziphora tenuior* [29], *Peganum harmala*, [30] *Annona reticulata* [31] and they showed various fabulous properties such as antibacterial, antimalarial and antiviral [32], anti-angiogenesis [33], anti-inflammatory [34], antiseptic sensors, treatment of cancer diagnosis [35]. *Antidesma Parvifolium* is a member of the Phyllanthaceae family, which is found in tropical Asia, Australia, and Africa. Since immemorial, the *Antidesma Parvifolium* herb has been used in traditional healthcare systems, particularly among tribal peoples. *Leaf* of *Antidesma* is used as an anti-headache, and the stem is used to stimulate menstrual flow and menorrhea. Also, leaf is used to increase breast milk production in women. *Antidesma* is mainly used for medicinal purposes. Hence, we have selected the *Antidesma Parvifolium* plant to produce Ag NPs, which serve as catalysts in the subsequent synthesis of heterocycles.

However, the disadvantages of most synthetic protocols for heterocyclic compounds include the employment of expensive catalysts, the catalyst's inability to be reused, the use of excess catalyst, the low yield of the final product, the prolonged reaction time, and the laborious workup. Hence, a catalytic system that is straightforward, effective, safe, and environmentally friendly is widely desired.

Recently, Azetidine scaffolds are convenient building blocks in heterocyclic chemistry [36-40]. Isoniazid (INZ) incorporated azetidine has grown tremendously in popularity in recent years due to the reports that numerous pharmacological compounds and pharmaceutical agents include the INZ scaffold as their primary structural component. Interesting biological behaviors they display include anti-inflammatory behaviors, antitubercular, anticonvulsant, antibacterial, etc. [41] Recently, one-pot multicomponent reactions, because of atom economy, it became a crucial tool in the synthesis of heterocyclic compounds, inexpensive, convenient, and simple workup [42, 43]. Various catalytic systems have been reported for the synthesis of azetidine, but they suffer from several limitations. One of the essential classes of organic heterocyclic compounds in a vast array of natural and synthetic products is isonicotinamide derivatives. Isonicotinamide exhibited a variety of pharmaceutical and medicinal activities like antimicrobial [44-46], antitubercular [47], cardiovascular [48], anticonvulsant [49], and anti-inflammatory activity [50]. Also, the literature survey reveals that various isonicotinamide derivatives were synthesized by using a $2\pi+2\pi$ cycloaddition one-pot multicomponent reaction [51-54] and a variety of catalysts such as $ZnCr_2O_4$, Montmorillonite K-10 [55-57], $SnCl_2$, piperidine [58]. A thorough literature review indicated that the $2\pi+2\pi$ cycloaddition reaction has only very seldom been investigated utilizing NPs catalyst [59].

In continuation of our previous work [60-67] Herein, we report Ag-NPs catalyzed one-pot three-component synthesis of *N*-(7-*R*)-2-oxa-6-azabicyclo[3.2.0]heptan-6-yl)isonicotinamide derivatives **(4a-h)**under ultrasonic irradiation.

2. Materials and Methods

2.1. Experimental

Without any additional purification, all of the chemicals were bought from Sigma Aldrich Laboratories. 5.5 L Ultrasonic bath (50Hz, 230V, and maximum temperature 70^{o}C), melting point were monitored on Electrothermal 9100 Apparatus. Using the KBr matrix, the FT-IR spectra were captured using a Brucker 3000 Hyperion Microscope and a Vertex 80 FTIR spectrometer. X-ray diffraction (XRD) measurements were performed on a Brucker AXS D8 advanced powder X-ray diffractometer using Cu-Kα radiation (λ = 1.5418 Å) and a 2^{o}/minute. Field Emission Scanning Electron Microscope (FESEM) was recorded on Carl Zeiss Supra 55 Germany equipment. ^{1}H and ^{13}C NMR spectra were noted on Bruker DRX-300, 400 MHz, and Vruker DRX-75, 100 MHz respectively. ESI-MS analyses were performed on the ESI-QTOF Analytical instrument. Using an Elementar Vario MICRO cube analyzer, elemental analysis was carried out. Thin-layer chromatography was used with aluminum sheets of silica gel 60F254 plates of 0.5 mm thickness and n-hexane:ethyl acetate (7:3) as the mobile phase to monitor the completion of reactions.

2.2. Preparation of Antidesma Parvifolium Leaf Powder.

Antidesma Parvifolium leaves were collected *Antidesma Parvifolium* plant (figure 1), Tertiary Magnon-Raigad, Maharashtra, India. Double distilled water was used to wash freshly collected *Antidesma Parvifolium* leaf. After the totally dried *leaves* were crushed and pulverized in a mixer, these leaves were sun-dried for 15 days. Finally, prepare homogenous dust-like powder.

Figure 1. *Antidesma Parvifolium* Plant.

2.3. Biosynthesis of Ag-NPs.

A mixture of homogenous *Antidesma Parvifolium leaf* powder (5 gm) and 100 ml double distilled water was irradiated under an Ultrasonication machine (230V AC, 50Hz power) for 10 minutes and cooled to room temperature. The reaction mixture was filtered through Whatman No. 1, and the resulting extract was utilized to create Ag NPs. It was then stored in a refrigerator at 4°C. The aqueous solution of Ag-NPs was poured into *Antidesma Parvifolium lea*f extract in a 1:1 ratio and kept for steady stirring on a magnetic stirrer at 600 rpm. After 20 minutes, the color of the reaction mixture turns brown. The resultant brown color mixture was centrifuged at room temperature using a centrifuge machine at 12,000 rpm. The residue was collected in a petri dish, dried for a few hours in the sun, and then the supernatant solution was discarded. Ultimately, the red powder, or Ag NPs, was produced. IR, ^{1}H NMR, and ^{13}NMR spectra are provided in the supplementary file (Figure S1 to Figure S14).

2.4. General Procedure for preparation of compounds (4a-h).

In a 25 ml round bottom flask, an equimolar combination of isoniazid (1 mmol) and aromatic aldehyde (1 mmol) was added, then a mixture of both 2,3-dihydrofuran (1 mmol) and Ag NPs catalyst (15 mol %) were successively added to the reaction mixture mentioned above was irradiated under 5.5 L ultrasonic bath for the appropriate time. TLC was used to monitor how the reaction was progressing. As soon as the response is finished, the catalyst was Ag-NPs were recovered by vacuum filtration technique and the crude products were obtained, and they were recrystallized using the appropriate solvents, using the standard workup technique.

2.5. Spectral data of synthesized isonicotinamide derivatives (4a-h)

2.5.1. N-(7-(phenyl)-2-oxa-6-azabicyclo[3.2.0]heptan-6-yl)isonicotinamide (4a).

Brownish yellow crystalline solid, M.P. 195-196°C. FTIR (KBr cm^{-1}): 3223(-NH), 2934(-CH), 1665(-C=O carbonyl), 1565(-C=C-aronatic); ^{1}H NMR (400 MHz, DMSO) δ 11.9 (s. 1H, D_2O exchangeable NH), 8.44-8.69 (m. 2H, Ar), 7.78 (m, 2H, Ar), 7.30-7.40 (m, 5H, Ar), 6.769 (m, 1H), 4.54 (m, 1H,), 3.07-3.21 (dd, 1H,), 3.72-3.80 (dd,1H), 3.20 (m, 1H), 2.50-2.56 (dd, 1H), 1.82-1.84 (dd, 1H); ^{13}C NMR (100 MHz, DMSO): 163.00, 149.93, 149.54, 140.79, 140.01, 129.89,128.53, 124.89, 121.02,12.03, 78.10, 76.00, 45.02, 40.00, 35.83.ppm; Mass : (M/Z) 295.13; Elemental Analysis: $C_{17}H_{17}N_3O_2$Calculated C= 69.14, H= 5.80, N= 14.23,; Found C= 69.09, H= 5.85, N=14.20.

2.5.2. N-(7-(4-cyanophenyl)-2-oxa-6-azabicyclo[3.2.0]heptan-6-yl)isonicotinamide (4b).

Yellow crystalline solid, M.P. 210-212°C. FTIR (KBr cm^{-1}): 3234(-NH), 2824 (-CH), 2261(-CN), 1656(-C=O Carbonyl), 1569 (-C=C Carbonyl); ^{1}H NMR (400 MHz, DMSO) δ 11.9 (s, 1H, D_2O exchangeable NH), 8.33-8.67 (m, 2H,Ar), 7.9 (m, 2H,Ar), 7.64-7.86 (m, 2H,Ar), 6.59-6.93 (m, 2H,Ar), 5.14 (m, 1H,), 4.60 (m, 1H,), 3.97-3.99 (dd, 1H,), 3.78-3.80 (dd,1H), 3.25 (m, 1H), 2.54-2.56 (dd, 1H), 1.81-1.83 (dd, 1H); ^{13}C NMR (100 MHz, DMSO): 162.19, 157.94, 149.98, 140.89, 135.40, 129.79, 123.68, 121.82, 119.29, 118.0, 113.59, 78.90, 76.80, 45.02, 40.00, 38.83..ppm; Mass : (M/Z) 320.13; Elemental Analysis: $C_{18}H_{16}N_4O_2$ Calculated C= 67.49, H= 5.03, N= 17.49; Found C= 67.41, H= 5.10, N=17.55.

2.5.3. N-(7-(2,5-dimethoxyphenyl)-2-oxa-6-azabicyclo[3.2.0]heptan-6-yl)isonicotinamide (4c).

White Crystalline solid, M.P. 192-195°C. FTIR (KBr cm^{-1}): 3234 (-NH), 2854 (-CH), 1655 (C=O carbonyl), 1575(-CH=CH-aromatic), 1060 (C-O, methoxy); ^{1}H NMR (400 MHz, DMSO) δ 11.92 (s, 1H, D_2O exchangeable NH), 8.67-8.78 (m, 2H,Ar), 7.7-7.81 (m, 2H,Ar), 7.48-7.49 (m, 1H,Ar), 6.88 (s, 1H,Ar), 6.84-6.87, (m, 1H,Ar), 5.10 (m, 1H,), 4.10 (m, 1H,), 3.97-3.99 (dd, 1H,), 3.78-3.80 (dd,1H), 3.26 (m, 1H), 3.8 (s, 6H), 2.56-2.58 (dd, 1H), 1.80-1.82 (dd, 1H); ^{13}C NMR (100 MHz, DMSO): 162.12, 153.67, 152.82, 150.25, 149.00, 140.70, 132.00, 123.65, 122.88, 118.43, 112.85, 110.07, 78.75, 56.28, 55.00, 40.00, 39.11. ppm; Mass: (M/Z) 355.32; Elemental Analysis: $C_{19}H_{21}N_3O_4$ Calculated C= 64.21, H= 5.96, N= 11.82; Found C= 64.09, H= 5.83, N= 11.93.

2.5.4. N-(7-(4-hydroxy phenyl)-2-oxa-6-azabicyclo[3.2.0]heptan-6-yl)isonicotinamide (4d).

Yellow crystalline solid, M.P. 224-226°C. FTIR (KBr cm^{-1}): 3288 (OH), 3231(-NH), 2839 (-CH), 1659 (-C=O Carbonyl), 1579 (-C=C- aromatic); ^{1}H NMR (400 MHz, DMSO) δ 11.6(s, 1H, D_2O exchangeable NH), 8.8-8.77 (m, 2H,Ar), 7.8 (m, 2H,Ar), 7.09 (m, 2H,Ar), 6.74 (m, 1H), 6.62 (m, 2H,Ar), 5.03 (s, 1H),4.85 (m, 1H,), 3.99-3.5 (dd, 1H,), 3.89 (dd,1H), 3.25 (m, 1H), 2.54 (dd, 1H), 1.81 (dd, 1H); ^{13}C NMR (100 MHz, DMSO): 163.37, 149.77, 154.12, 140.69, 132.40, 129.02, 126.80, 121.02, 106.02, 77.00, 76.05, 45.32, 40.25, 33.12. ppm; Mass: (M/Z) 311.14; Elemental Analysis: $C_{17}H_{17}N_3O_3$Calculated C= 65.58, H= 5.50, N= 13.50; Found C= 65.52, H= 5.52, N=13.48.

2.5.5. N-(7-(3-bromophenyl)-2-oxa-6-azabicyclo[3.2.0]heptan-6-yl)isonicotinamide (4e).

Orange crystalline solid, M.P. 183-185°C. FTIR (KBr cm^{-1}): 3236(-NH), 2914(-CH), 1635(-C=O carbonyl), 1571(-C=C- aromatic); ^{1}H NMR (400 MHz, DMSO) δ 11.7(s, 1H, D_2O exchangeable NH), 8.40-8.67 (m, 2H,Ar), 7.9 (m, 2H,Ar), 7.56 (s, 1H,Ar), 7.23-7.50 (m, 3H,Ar), 6.75 (m, 1H),4.85 (m, 1H,), 3.99-3.5 (dd, 1H,), 3.89 (dd,1H), 3.25 (m, 1H), 2.54 (dd, 1H), 1.81 (dd, 1H); ^{13}C NMR (100 MHz, DMSO): 162.27, 149.87, 146.25, 140.69, 136.40, 130.19, 129.28, 126.80, 110. 12, 78.10, 76.25, 45.02, 40.00, 36.93. ppm; Mass: (M/Z) 373.05; Elemental Analysis: $C_{17}H_{16}BrN_3O_2$ Calculated C= 54.56, H= 4.31, N= 11.23; Found C= 54.41, H= 4.40, N=11.31.

2.5.6. N-(7-(4-chlorophenyl)-2-oxa-6-azabicyclo[3.2.0]heptan-6-yl)isonicotinamide (4f).

Whitish crystalline solid, M.P. 189-192°C. FTIR (KBr cm^{-1}): 3201(-NH), 2841(-CH), 1685(-C=O carbonyl), 1555(-C=C- aromatic); ^{1}H NMR (400 MHz, DMSO) δ 11.8 (s, 1H, D_2O exchangeable NH), 8.86 (m, 2H,Ar), 7.83 (m, 2H,Ar), 7.47 (m, 2H,Ar), 7.39 (m, 2H,Ar), 6.69 (m, 1H),4.80 (m, 1H,), 3.80-3.73 (dd, 1H,), 3.88 (dd,1H), 3.02 (m, 1H), 2.23 (dd, 1H), 1.51 (dd, 1H); ^{13}C NMR (100 MHz, DMSO): 162.87, 149.87, 140.93, 138.40, 130.15, 129.12, 128.56, 126.80, 121.78, 105.02, 77.02, 75.65, 44.82, 40.35, 32.72. ppm; Mass: (M/Z) 329.08; Elemental Analysis: $C_{17}H_{16}ClN_3O_2$, Calculated C= 61.91, H= 4.89, N= 12.74; Found C= 61.95, H= 4.90, N=12.72.

2.5.7. N-(7-(3-hydroxy,4-methoxyphenyl)-2-oxa-6-azabicyclo[3.2.0]heptan-6-yl)isonicotinamide(4g).

Yellow crystalline solid, M.P. 176-178°C. FTIR (KBr cm^{-1}): 3223(-NH), 2814 (-CH), 1660 (-C=O carbonyl), 1570(-C=C- aromatic); ^{1}H NMR (400 MHz, DMSO) δ 11.9 (s, 1H, D_2O exchangeable NH), 8.69-8.81 (m, 2H,Ar), 7.79-8.0(m, 2H,Ar), 7.5 (s, 1H Ar), 7.3 (m, 2H,Ar), 5.20 (s, 1H,), 5.11 (m, 1H,), 4.10 (m, 1H,), 3.97-3.96 (dd, 1H,), 3.75-3.79 (dd,1H), 3.26 (m, 1H), 3.78 (s, 1H), 2.46-2.58 (dd, 1H), 1.81-1.82 (dd,1H); ^{13}C NMR (100 MHz, DMSO): 162.23, 149.43, 150.24, 148.9, 145.13, 140.34, 135.13, 131.61, , 122.71, 120.70, 113.16, 77.10, 76.0, 56.04, 41.38, 40.32, 39.09. ppm; Mass: (M/Z) 341.14; Elemental Analysis: $C_{18}H_{19}N_3O_4$, Calculated C= 63.33, H= 5.61, N= 12.31; Found C= 63.41, H= 5.59, N=12.33.

2.5.8. N-(7-(3,4-dihydroxyphenyl)-2-oxa-6-azabicyclo[3.2.0]heptan-6-yl)isonicotinamide (4h).

White Crystalline solid, M.P. 132-135°C. FTIR (KBr cm^{-1}): 3320 (-OH al), 3210 (-NH), 2829 (-CH), 1644(-C=O carbonyl), 1535 (-C=C- aromatic); ^{1}H NMR (400 MHz, DMSO) δ 12.2 (s, 1H, D_2O exchangeable NH), 8.67-8.80 (m, 2H,Ar), 7.80-8.0(m, 2H,Ar), 7.4 (s, 1H Ar), 7.3 (m, 2H,Ar), 5.30 (s, 2H,), 5.10 (m, 1H,), 4.10 (m, 1H,), 3.97-3.99 (dd, 1H,), 3.78-3.80 (dd,1H), 3.26 (m, 1H), 2.56-2.58 (dd, 1H), 1.80-1.82 (dd, 1H); ^{13}C NMR (100 MHz, DMSO): 162.26, 150.43, 149.91, 148.9, 144.43, 140.64, 136.13, 130.61, 128.56, 123.71, 121.81, 113.06, 78.00, 77.10, 41.38, 40.32, 39.09. ppm; Mass: (M/Z) 327.119; Elemental Analysis: $C_{17}H_{17}N_3O_4$, Calculated C= 62.28, H= 5.23, N= 12.84; Found C= 62.31, H= 5.15, N=12.79.

3. Result and Discussion

3.1. Biological Evaluation.

Antibacterial activity Biosynthesized Ag-NPs were examined utilising the Disc Diffusion Technique, and the media employed was Agar PDA [68]. Examining synthetic Ag NPs against Staphylococcus aureus, *Escherichia Coli, and Spedomonous Aruginosa* stains with Gentamycin as a standard.

3.2. X-ray diffraction Analysis.

The typical analytical method for determining the crystal size, crystal plane, and crystal structure of a nanomaterial is the XRD pattern. Ag-NPs may be thoroughly penetrated by X-rays, which can reveal information about their size and crystal structure. Synthesized biogenic Ag-NPs were confirmed through the X-diffraction approach (figure 2). The face center cubic (FCC) pattern of Ag corresponding to (111), (200), (220), (311) and (222) planes, as well as corresponding diffraction peaks (2Θ) = 38.1°, 44.3°, 64.4°, 77.44° and 81.58° was confirmed with standard JCPDS file No. 96-900-8460. The Debye Scherrer formula also predicts that produced Ag-NP crystals have a size of about 21 nm [69].

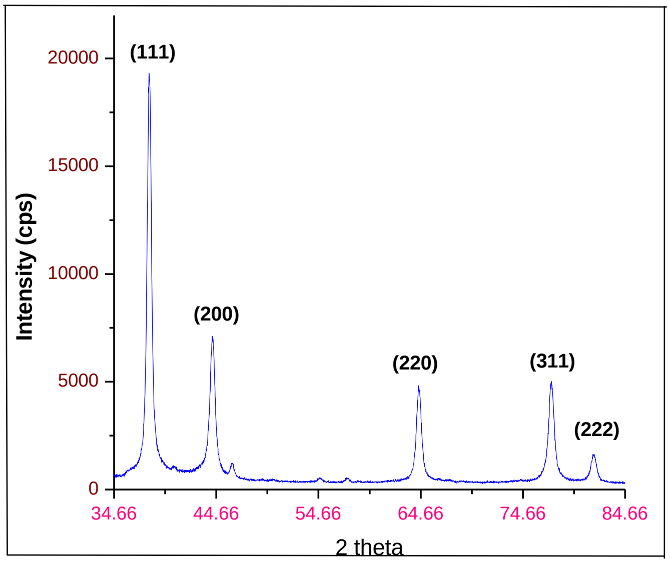

Figure 2. X-ray diffraction for Ag NPs.

3.3. FTIR Analysis of Ag-NPs.

The biomolecule-derived functional groups that are involved in the biosynthesis of Ag-NPs were found using the FTIR approach (figure 3). The FTIR frequency at 3369.99 cm^{-1} reveals the existence of the phenolic/alcoholic -OH group, whereas 1594.87 cm^{-1} indicates the presence of carbonyl group (C=O), 1384 cm^{-1} frequency showed aromatic compounds containing C=C functional group and 1110 cm^{-1} frequency displayed C-O stretching. This FTIR frequency confirms the major supposition regarding the existence of phytochemicals involved in the production of Ag-NPs.

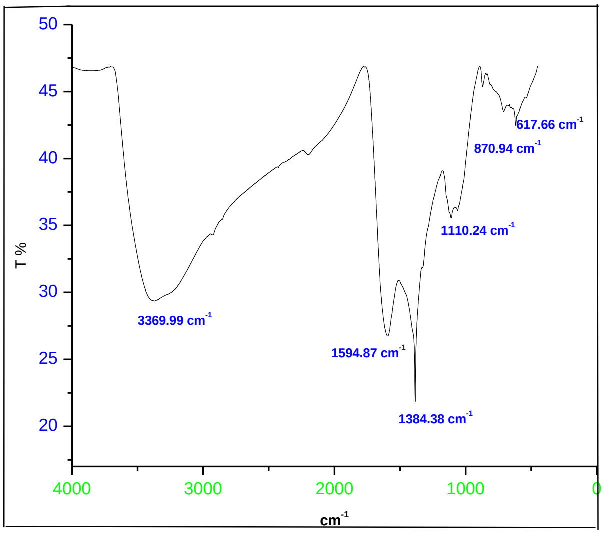

Figure 3. FT-IR of Ag NPs.

3.4. EDS Analysis.

The EDS investigation revealed that the produced Ag NPs were pure (figure 4). Silver showed a significant signal at an energy level of 3.3 KeV, while weak signals from O, Ca, Mg, Rb, Na, and K were also seen. The major emission energy for silver was found at 3.3 KeV.

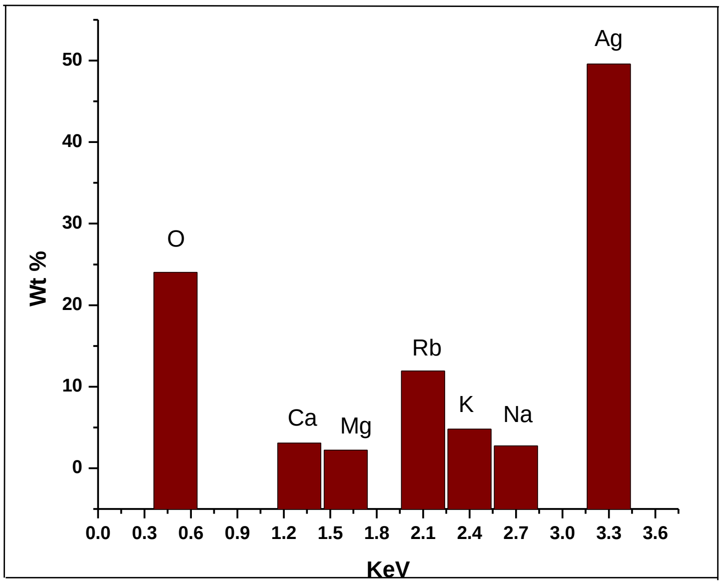

Figure 4. EDS pattern of Ag NPs

FESEM study: FESEM (figure 5) investigation is applied to characterize the shape, size, and morphology of the biosynthesized Ag-NPs from *Antidesma Parvifolium* leaf extract. The resulting FESEM images of Ag-NPs exhibit spherical morphologies with 21nm particle sizes.

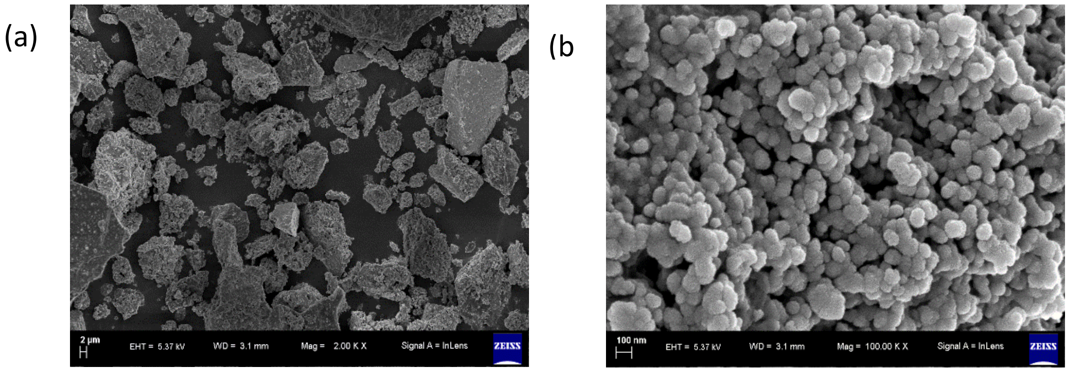

Figure 5. FESEM morphological images (a) and (b) for Ag NPs.

3.5. Applications of Ag NPs.

Metallic NPs have shown prominent results against antibacterial strains [70], Simultaneously, one of the most traditional and environmentally friendly methods for creating bioactive nano catalysts is by the production of synthetic NPs from plant extracts. In particular, the presence of many phytochemicals in the *Antidesma Parvifolium* plant extract can increase the stability and activity of Ag-NPs. Actually, AG-NPs are extremely noxious to microorganisms and display considerable antibacterial properties [71]. The great bioactivity of Ag-NPs can be ascribed to their small sizes and excessive surface area [72]. Comparably, biosynthesize Ag-NPs (Table 1) have a small size and a high surface area, and they significantly outperform standard Gentamycin in terms of antibacterial activity against Staphylococcus aureus (15 mm zone of inhibition), *Spedomonous Aruginosa* (14 mm zone of inhibition), and Escherichia coli (12 mm zone of inhibition) (18 mm).

Table 1. Antibacterial Properties of prepared Ag NPs.

Pathogenic Bacterial Stain	Ag NPs (Zone of inhibition in mm)	Reference (Zone of inhibition in mm)
Staphylococcus aureus	15	18
Escherichia Coli	12	18
Spedomonous Aruginosa	14	18

Synthesis of N-(7-R)-2-oxa-6-azabicyclo[3.2.0]heptan-6-yl)isonicotinamide derivatives: Heterocyclic compounds with isoniazid incorporation have garnered a lot of attention due to their numerous medicinal uses. It prompted our interest to design and developed an eco-friendly, efficient, robust protocol for isonicotinamide derivatives synthesis. Nowadays, several researchers reported improved methods for the synthesis of isoniazid-based heterocyclic compounds, but most of them are conventional, expensive, tedious, unstable multi-steps, and contain hazardous organic solvents. Hence to overcome these several issues we design and developed Ag-NPs from *Antidesma Parvifolium plant* extract and used them as catalysts in our present synthesis.

The synthesis of *N*-(7-*R*)-2-oxa-6-azabicyclo[3.2.0]heptan-6-yl)isonicotinamide derivatives **(4a-h)** was archived by one-pot three-component cycloaddition using Ag NPs as a catalyst and ultrasonic irradiation at 70°C, the reaction of isoniazid (1), substituted aromatic aldehydes (2a-h), and 2,3 dihydrofuran (3) produces the product in excellent yields (Table 2).

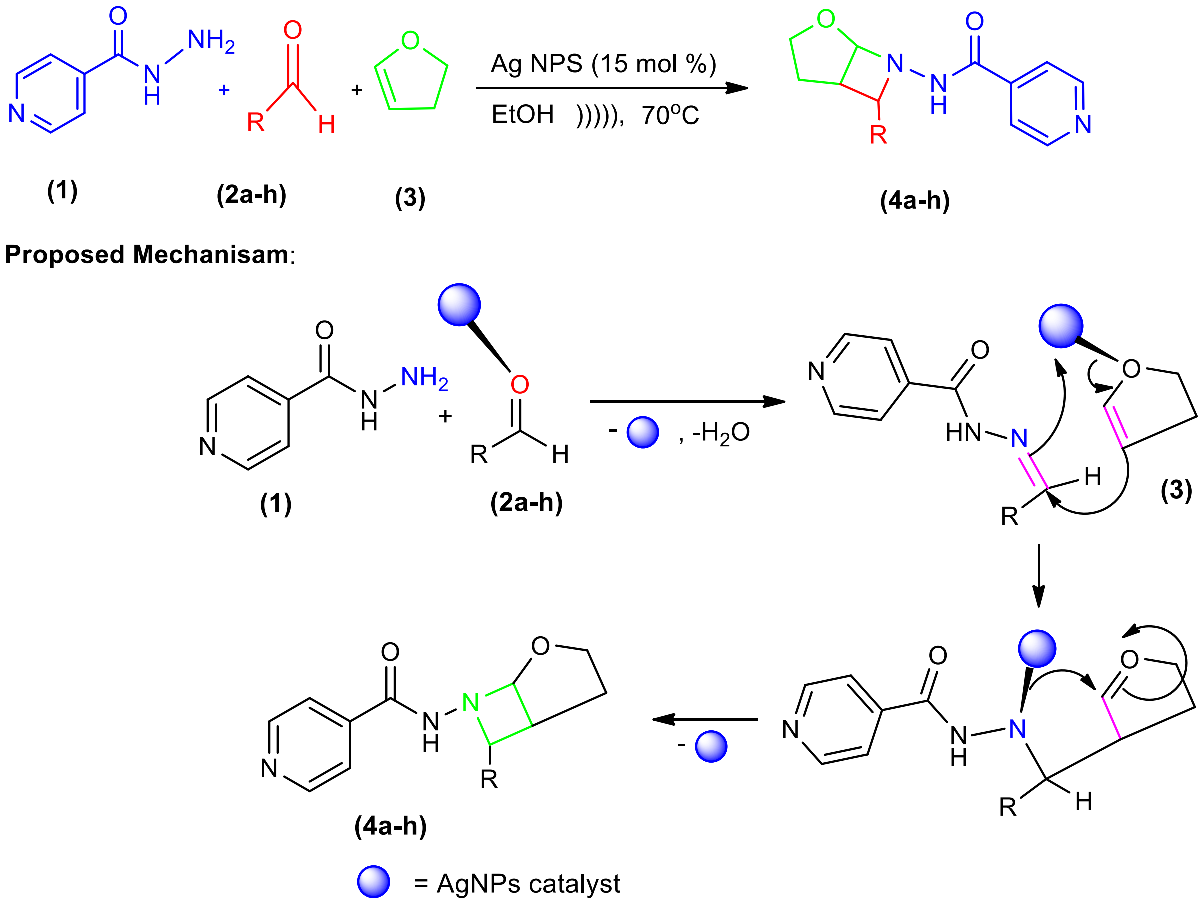

Scheme 1. Synthesis scheme with Proposed mechanism for the synthesis of isonicotinamide derivatives (4a-h) using Ag NPs catalyst.

For the model studies, Isoniazid (**1**), benzaldehyde (**2a**) were used in order to test the reaction conditions, 2,3 dihydrofuran (**3**) was utilised as the aldehyde components and as the model reaction. In addition to searching for the best solvent, the reaction was examined using different solvents, namely methanol, ethanol, acetonitrile, and chloroform, in different proportions using Ag NPs as a catalyst under ultrasonic irradiation. Table 2 provides a summary of the outcomes. Even though the reaction proceeded without issue in each of the chosen solvents, the use of ethanol resulted in a consistently higher yield (89%).

Table 2. Optimization of solvent, catalyst, and temperature for the Synthesis of N-(7-Phenyl)-2-oxa-6-azabicyclo[3.2.0]heptan-6-yl)isonicotinamide derivatives.

Entry	Solvent	US Temp. (°C)	Catalyst (mol %)	Time (hrs)	Yields(%)[a]
1	MeOH	70	15	2.30	85
2	CH_3CN	70	15	2.30	61
3	$CHCl_3$	70	15	2.30	56
4	EtOH	35	15	2.30	20
5	EtOH	50	15	2.30	78
6	**EtOH**	**70**	**15**	**2.30**	**89**
7	EtOH	70	05	2.30	54
8	EtOH	70	10	2.30	81
9	EtOH	70	20	2.30	90

[a] Isolated yield.

Furthermore, we discovered the possibility of recycling the Ag-NPs (figure 6). The NPs were recovered from the model reaction by filtration and checked in the subsequent run without purification. After four successive runs, the activity of the catalyst does not get much, but up to four cycles (cycle 1: 94%, cycle 2: 92%, cycle 3: 88%, and cycle 4: 83%), recovery of NPs was good.

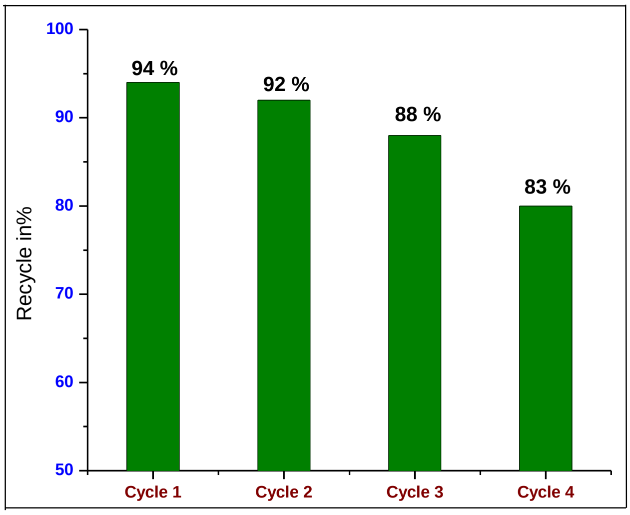

Figure 6. Successive cycles of Ag NPs.

Several concentrations were used to carry out the reaction of the Ag-NPs as a catalyst (5 to 20 mol %) for the synthesis of isonicotinamide derivatives **(4a-h)**. The product of yield increases from 54 % to 90 % in conjunction with an increase in NPs catalyst concentration

(Table 3). The highest percentage of product yield was achieved with the 15 mol% catalyst due to the ultrasonic effect, which was followed by a modest rise in product yield with the 20 mol% catalyst. Therefore, the 15 mol% Ag-NPs catalyst was selected for all subsequent reactions of *N*-(7-*R*)-2-oxa-6-azabicyclo [3.2.0] heptan-6-yl) isonicotinamide derivatives **(4a-h)**. The influence of different temperatures (35°C, 50 °C, and 70°C) of ultrasonication was investigated in a reaction. The 70°C temperature displayed the highest percentage of product yield (Entry 6, Table 2).

Table 3. Ag NPs catalyzed synthesis of N-(7-R)-2-oxa-6-azabicyclo[3.2.0]heptan-6-yl)isonicotinamide derivatives **(4a-h).**

Entry	R	Product	Time (hrs)	Yields(%)[a]
1.	Ph	4a	2.30	89
2.	4-CNC_6H_4	4b	2.35	84
3.	2,5-$(MeO)_2C_6H_3$	4c	2.27	90
4.	4-HOC_6H_4	4d	2.40	88
5.	3-BrC_6H_4	4e	2.25	85
6.	4-ClC_6H_4	4f	2.38	89
7.	3-HO-4-$MeOC_6H_3$	4g	2.29	87
8.	3,4-$(HO)_2C_6H_3$	4h	2.32	86

(Reaction condition: isoniazide (1 mmol), aromatic aldehyde (1 mmol), 2,3-dihydrofuram (1 mmol) and Ag NPs (15 mol %) catalyst in ethanol solvent (6 ml) at 70°C under ultrasonic irradiation).

[a] Isolated yield.

The reaction of substituted aromatic aldehydes **(2a-h)** was smoothly channelized under the optimal reaction conditions, carried out, and provided predicted products in good to excellent yields (84-90%) under the ultrasonic irradiation technique (Table 3). Those experiments allowed us to invent a new cascade process, which results in the formation of *N*-(7-*R*)-2-oxa-6-azabicyclo[3.2.0]heptan-6-yl)isonicotinamide derivatives **(4a-h)** in a single step. The condensation between isoniazid with substituted aromatic aldehyde leads to the formation of Schiff base, which subsequently undergoes the cyclization with 2,3-dihydrofuram in the presence of AG-NPs under ultrasound irradiation in the same pot. The current synthetic method, however, continues to be a helpful and straightforward protocol for the creation of a broad range of molecules in this family.

4. Conclusion

In conclusion, we have precisely illuminated the biosynthesis and antimicrobial performance of 21nm size spherical shape Ag-NPs from *leaf* extract of *Antidesma Parvifolium* plant and its catalytic application in heterocyclic synthesis. The synthetic method demonstrated the enormous potential of Ag NPs as a catalyst for the synthesis of several sophisticated heterocyclic molecules. This approach has certain remarkable qualities that are appealing, especially in terms of green chemistry, non-hazardous nature, simplicity, ease of workability, easy separation, excellent catalytic activity, recyclability of Ag-NPs because of their efficiency and reusability in the organic synthesis process, atom economy, high yields (84-90%), and replacement of multi-step synthesis by a one-pot multicomponent reaction.

Funding

This research received no external funding.

Acknowledgments

We are appreciative that the principal of the Doshi Vakil Arts College & G.C.U.B. Science College, Goregaon-Raigad, India, provided the essential research facilities.

Conflicts of Interest

The authors announce no conflict of attentiveness.

References

1. Ju-Nam, Y.; Lead, J.; Manufactured nanoparticles: An overview of their chemistry, interactions and potential environmental implications. *Science of the Total Environment.* **2008**, *400*, 396-414. https://doi.org/10.1016/j.scitotenv.2008.06.042
2. Daniel, M. C.; Astruc, D.; Gold Nanoparticles: Assembly, Supramolecular Chemistry, Quantum-Size-Related Properties, and Applications toward Biology, Catalysis, and Nanotechnology. *Chem. Rev.* **2004**, *104*, 293–346. https://doi.org/10.1021/cr030698+
3. Chaudhari, R. G.; Paria, S.; Core/Shell Nanoparticles: Classes, Properties, Synthesis Mechanisms, Characterization, and Applications. *Chem. Rev.* **2012**, *112*, 2373–2433. https://doi.org/10.1021/cr100449n
4. Ahmed, S.; Zafeer, A. I.; Ikram, S.; One-Step Method for Formation of Silver Nanoparticles Using Withania somnifera Extract for Antimicrobial Activities. *J. Bionanosci.* **2016**, *10(1)*, 47–53. https://doi.org/10.1166/jbns.2016.1356
5. Frewer, L. J.; Gupta, N.; George, S.; Fischer, A. R. H.; Giles, E. L.; Coles, D.; Consumer attitudes towards nanotechnologies applied to food production. *Trends. Food Sci. Technol.* **2014**, *40*, 211–225. http://dx.doi.org/10.1016/j.tifs.2014.06.005
6. Parveen, M.; Ahmad, F.; Malla, A. M.; Azaz, S.; Microwave-assisted green synthesis of silver nanoparticles from Fraxinus excelsior leaf extract and its antioxidant assay. *Applied Nanoscience.* **2015**, *6(2)*, 267–276. https://doi.org/10.1007/s13204-015-0433-7
7. Song, J. Y.; Kim, B. S.; Rapid biological synthesis of silver nanoparticles using plant leaf extracts. *Bioprocess and Biosystems Engineering.* **2008**, *32(1)*, 79–84. https://doi.org/10.1007/s00449-008-0224-6
8. Murugan, A.; Shanmugasundaram, K. K.; *In vitro*: phytochemical screening and evaluation of antioxidant potential of vitex negundo. linn of synthesized silver nanoparticles. *World J. Pharm. Pharm. Sci.* **2014**, *3(10)*, 855–868. https://www.wjpps.com/Wjpps_controller/abstract_id/2129
9. Sedaghat, S.; Agbolag, A. E.; Bagheriyan, S.; Biosynthesis of silver nanoparticles using pennyroyal water extract as a green route. *J. Nanostructure in Chem.* **2015**, *6(1)*, 25–27. https://doi.org/10.1007/s40097-015-0176-8
10. David, L.; Moldovan, B.; Vulcu, A.; Olenic, L.; Perde-Schrepler, M.; Fischer-Fodor, E.; Filip, G. A.; Green synthesis, characterization and anti-inflammatory activity of silver nanoparticles using European black elderberry fruits extract. *Biointerfaces*, **2014**, *122*, 767–777. https://doi.org/10.1016/j.colsurfb.2014.08.018
11. Sadowski, Z.; Maliszewska, I, H.; Grochowalska, B.; Polowczyk, I.; Kozlecki, Synthesis of silver nanoparticles using microorganisms. *Mater. Sci-Poland,* **2008**, *26(2)*, 419–424. https://www.researchgate.net/profile/Tomasz-Kozlecki/publication/228411163_Synthesis_of_silver_nanoparticles_using_microorganisms/links/0fcfd50fc26103e8fe000000/Synthesis-of-silver-nanoparticles-using-microorganisms.pdf
12. Tsibakhashvili, N.; Kalabegishvili, T.; Gabunia, V.; Gintury, E.; Kuchava, N.; Bagdavadze, N.; Pataraya, D.; Gurielidzse, M.; Gvarjaladze, D.; Lomidze, L.; *Nano Studies*. **2010**, *2*, 179–182.
13. Korbekandi, H.; Ashari, Z.; Iravani, S.; Abbasi, S.; Optimization of Biological Synthesis of Silver Nanoparticles using Fusarium oxysporum. *Iran. J. Pharm. Res.*, **2013**, *12(3)*, 289–298. https://pubmed.ncbi.nlm.nih.gov/24250635/

14. Mahendran, G.; Ranjitha Kumari, B. D.; Biological activities of silver nanoparticles from Nothapodytes nimmoniana (Graham) Mabb. fruit extracts. *Food Science and Human Wellness*,**2016**, *5(4)*, 207–218. https://doi.org/10.1016/j.fshw.2016.10.001
15. Jemal, K.; Sandeep, B. V.; Pola, S.; Synthesis, Characterization, and Evaluation of the Antibacterial Activity of Allophylus serratus Leaf and Leaf Derived Callus Extracts Mediated Silver Nanoparticles. *Journal of Nanomaterials*, **2017**, 1–11. https://doi.org/10.1155/2017/4213275
16. Heydari, R.; Rashidipour, M.; Green Synthesis of Silver Nanoparticles Using Extract of Oak Fruit Hull (Jaft): Synthesis and In Vitro Cytotoxic Effect on MCF-7 Cells. *International Journal of Breast Cancer*. **2015**, 1–6. https://doi.org/10.1155/2015/846743
17. Bar, H.; Bhui, D. K.; Sahoo, G. P.; Sarkar, P.; Pyne, S.; Misra, A.; Green synthesis of silver nanoparticles using seed extract of Jatropha curcas. *Physicochem. Engin. Aspects.* **2009**, *348(1-3)*, 212–216. https://doi.org/10.1016/j.colsurfa.2009.07.021
18. Ahmed, S.; Ahmad, M.; Swami, B. L.; Ikram, S.; A review on plants extract mediated synthesis of silver nanoparticles for antimicrobial applications: A green expertise. *J. Adv. Res.* **2016**, *7*, 17–28. https://doi.org/10.1016/j.jare.2015.02.007
19. Baghizadeh, A.; Ranjbar, S.; Gupta, Asif, V. K.; Pourseyedi, M. S.; Karimi, M. J.; Mohammadinejad, M.; Green synthesis of silver nanoparticles using seed extract of Calendula officinalis in liquid phase. *J. Mol. Liquids*. **2015**, *207*, 159-163. https://doi.org/10.1016/j.molliq.2015.03.029
20. Fierascu, I.; Bunghez, I. R.; Fierascu, R. C.; Ion, M. C.; Dinu-Pirvu, C. E.; Nuţa, D. F.; Characterization and antioxidant activity of phytosynthesised silver nanoparticles using calendula officinalis extract. *Farmacia* **2014**, *62(1)*, 129–136. https://farmaciajournal.com/wp-content/uploads/2014-01-art-12-fierascu-129-136.pdf
21. Azizi, M.; Sedaghat, S.; Tahvildar, K.; Derakhshi, P.; Ghaemi, A.; Synthesis of silver nanoparticles using Peganum harmala extract as a green route. *Green Chem. Lett. Rev.* **2017**, *10(4)*, 420–427. https://doi.org/10.1080/17518253.2017.1395081
22. Mehmood, A.; Murtaza, C.; Bhatti, T. M.; Kausar, R.; Phyto-mediated synthesis of silver nanoparticles from Melia azedarach L. leaf extract: characterization and antibacterial activity. *Arab. J. Chem.* **2017**, *10*, S3048–S3053. https://doi.org/10.1016/j.arabjc.2013.11.046
23. Mohammadinejad, R.; Pourseyedi, S.; Baghizadeh, A.; Ranjbar, S.; Mansoori, G. A. Synthesis of Silver Nanoparticles Using Silybum Marianum Seed Extract. *Int. J. Nanosci. Nanotechnol.* **2013**, *9(4)*, 221–226. http://trl.lab.uic.edu/1.OnlineMaterials/nano.publications/13.AgNP_Using_Silybum_Marianum.pdf
24. Rahimi, Z.; Yousefzadi, M.; Noori, A.; Akbarzadeh, A.; *J. Persian Gulf*. **2014**, *5(15)*, 9-15. https://www.researchgate.net/publication/330740756_Green_Synthesis_of_Silver_Nanoparticles_using_Ulva_flexousa_from_the_Persian_Gulf_Iran
25. Vijayan, R.; Joseph, S.; Mathew, B.; Green synthesis of silver nanoparticles using Nervalia zeylanica leaf extract and evaluation of their antioxidant, catalytic, and antimicrobial potentials. *Part. Sci. Technol*. **2018**, *37(7)*, 1–11. https://doi.org/10.1080/02726351.2018.1450312
26. Reddy, N.V.; Satyanarayana, B. M.; Sivasankar, S.; Eco-friendly synthesis of silver nanoparticles using leaf extract of Flemingia wightiana: spectral characterization, antioxidant and anticancer activity studies. *SN Appl. Sci.* **2020**, *2*, 884, https://doi.org/10.1007/s42452-020-2702-7
27. Pande, S. N.; Bharati, K. T.; Wakchure, S. K.; Ghotekar, S. K.; Gujrathi, D. B.; Phatangare, N. D.; Green synthesis of silver nanoparticles by caralluma fimbriata L. and its characterization. *Indian. J. App. Res.* **2015**, *5(2)*, 749–750. https://doi.org/10.36106/ijar
28. Patanayak, S.; Mollick, M. M. R.; Maity, D.; Chakraborty, S.; Dash, S. K.; Roy, S.; Chattopadhay, S.; Chattopadhay, D.; Chakraborty, M.; Butea monosperma bark extract mediated green synthesis of silver nanoparticles: Characterization and biomedical applications. *J. Saudi. Chem. Soc.* **2017**, *21*, 673–684. https://doi.org/10.1016/j.jscs.2015.11.004
29. Moteria, P.; Chanda, S.; Synthesis and characterization of silver nanoparticles using Caesalpinia pulcherrima flower extract and assessment of their in vitro antimicrobial, antioxidant, cytotoxic, and genotoxic activities. *Artif. Cells Nanomed. Biotechnol. 45*, **2017**, 1556–1567. https://doi.org/10.1080/21691401.2016.1261871
30. Carmona, E. R.; Benito, N.; Plaza, T.; Recio-Sánchez, G.; Green synthesis of silver nanoparticles by using leaf extracts from the endemic Buddleja globosa hope. *Green Chem. Lett. Rev.***2017**, *10*, 250–256. https://doi.org/10.1080/17518253.2017.1360400

31. Kumar, B.; Smita, K.; Cumbal, L. Debut, A.; Sacha inchi (Plukenetia volubilis L.) shell biomass for synthesis of silver nanocatalyst. *J. Saudi. Chem. Soc.* **2017**, *21*, S293–S298. https://doi.org/10.1016/j.jscs.2014.03.005
32. Elechiguerra, J. L.; Burt, J. L.; Morones, J. R.; Camacho-Bragado, A.; Gao, X.; Lara, H. H.; Yacaman, M. J.; Interaction of silver nanoparticles with HIV-1. *J. Nanobiotechnol.* 3(6), **2005**, https://doi.org/10.1186/1477-3155-3-6
33. Gurunathan, S.; Lee, K. J. Kalishwaralal, K.; Sheikpranbabu, S.; Vaidyanathan, R.; Eom, S. H.; *Biomaterials*, **2009**, *30*, 6341–6350. https://doi.org/10.1016/j.biomaterials.2009.08.008
34. Nadworny, P. L.; Wang, J.; Tredget, E. E.; Burrell, R. E.; Anti-inflammatory activity of nanocrystalline silver in a porcine contact dermatitis model. *Nanomedicine*, **2008**, *4*, 241–251. https://doi.org/10.1016/j.nano.2008.04.006
35. Popescu, M.; Velea, A.; Lorinczi, A.; Biogenic production of nanoparticles. *Dig. J. Nanomater. Biostruct.* **2010**, *5*, 1035–1040. https://chalcogen.ro/1035_Popescu.pdf
36. Chang, M. W.; Giffin, M. J.; Muller, R.; Savage, J.; Lin, Y. C.; Hong, S.; Jin, W.; Whitby, L.R.; Elder, J. H.; Boger, D. L.; Torbett, B. E.; Identification of Broad-Based HIV-1 Protease Inhibitors From Combinatorial Libraries. *Biochem J.* **2010**, *429(3)*, 527–532. https://doi.org/10.1042/BJ20091645
37. Brewster, J.T.; Randall, S.D.; Kowalski, J.; Cruz, C.; Shoemaker, R.; Tarlton, E.; Hinklin, R.J.; A Decarboxylative Cross-Coupling Platform To Access 2-Heteroaryl Azetidines: Building Blocks with Application in Medicinal Chemistry. *Organic Letters*. **2022**, https://doi.org/10.1021/acs.orglett.2c03852
38. Shukla, P.; Deswal, D.; Narula, A.K.; Monomeric silica supported interaction of TOSMIC with highly functionalized imines: A green approach to azetidines via ABB-type cycloaddition reaction. *J. Het. Chem.*, **2022,** *59*(11), 2037-2046. https://doi.org/10.1002/jhet.4526
39. Becker, M. R.; Wearing, E. R.; Schindler, C. S.; Synthesis of azetidines via visible-light-mediated intermolecular [2+ 2] photocycloadditions. *Nature Chemistry*, **2020**, *12*(10), 898-905. https://doi.org/10.1038/s41557-020-0541-1
40. Schafer, C.; Cho, H.; Vlocsko, B.; Xie, G.; Torok, B.; Recent Advances in the Green Synthesis of Heterocycles: From Building Blocks to Biologically Active Compounds. *Curr. Org. Syn.* **2022,** *19*(3), 426-462. https://doi.org/10.2174/1570179418666210910110205
41. Chavan, P.; Jadhav, S.; Farooqui, M.; Rai, M.; Biological Significance of Ultrasound Assisted Synthesized Polycyclic Azetidine Derivatives. *Poly. Aro.Comps.* **2020**, *42(4)*, 999-1012. https://doi.org/10.1080/10406638.2020.1764983
42. Chandrasekhar, S.; Narsihmulu, C.; Chandrasekhar, G.; Shyamsunder, T.; Pd/$CaCO_3$ in liquid poly (ethylene glycol) (PEG): an easy and efficient recycle system for partial reduction of alkynes to cis-olefins under a hydrogen atmosphere. *Tet. Lett.* **2004**, *45*, 2421–2423. https://doi.org/10.1016/j.tetlet.2004.01.097
43. Gupta, S.; Khanna, G.; Khurana, J. M.; A facile eco-friendly approach for the one-pot synthesis of 3,4-dihydro-2H-naphtho[2,3-e][1,3]oxazine-5,10-diones using glycerol as a green media. *Environ. Chem. Lett.* **2016**, *14*, 559–564. https://doi.org/10.1007/s10311-016-0570-6
44. Srivastava, S. K.; Dua, R.; Srivastava, S. D.; Synthesis and antimicrobial activity of [N1-(N-substitutedarylidene-hydrazino)-acetyl]-2-methyl-imidazoles and [N1-(4-substituted aryl-3-chloro-2-oxo-1-azetidinyl-amino)-acetyl]-2-methyl-imidazoles. *Proc. Nat. Acad. Sci. India, Sec. A: Phys. Sci.*, **2010**, *80*, 117-121.
45. Trivedi, P. B.; Synthesis and antimicrobial activity of 4-oxothiazolidines, Azetidino-2-ones, malonanilic acidhydrazines and pyrazoline derivatives of phenothiazine. *Undavia. Indian J. Chem.* **1993**, *32B(7)*, 760-765.
46. Panwar, H.; Verma, R. S.; Srivastava, V. K.; Kumar, A.; Synthesis of some substituted azetidinonyl and thiazolidinonyl-1,3,4-thiadiazino[6,5-b]indoles as prospective antimicrobial agents. *Indian J. Chem.* **2006**, *45B*, 2099-2104. http://nopr.niscpr.res.in/bitstream/123456789/6682/1/IJCB%2045B(9)%202099-2104.pdf
47. Patel, R. B.; Desai, P. S.; Desai, K. R.; Chikhalia. K. H.; Synthesis of pyrimidine based thiazolidinones and azetidinones: Antimicrobial and antitubercular agents. *Indian. J. Chem.* **2006**, *45B*, 773-778. https://nopr.niscpr.res.in/bitstream/123456789/6394/1/IJCB%2045B%283%29%20773-778.pdf
48. Akihisa, T.; Mafune, S.; Ukiya, M.; Kimura, Y.; Yasukawa, K.; Suzuki, T.; Tokuda, H.; Tanabe, N.; Fukuoka. T.; (+)- and (−)-syn-2-Isobutyl-4-methylazetidine-2,4-dicarboxylic Acids from the Extract of Monascus pilosus-Fermented Rice (Red-Mold Rice). *J. Nat. Prod.* **2004**, *67(3)*, 479-480. https://doi.org/10.1021/np030394i

49. Couty, F.; Gwilherm, E.; Azetidines: New Tools for the Synthesis of Nitrogen Heterocycles. *Syn. Lett.* **2009**, *19*, 3053-3064. https://doi.org/10.1055/s-0029-1218299
50. Siddiqui, N.; Rana, A.; Khan, S. A.; Haque, S. E.; Alam, M. S.; Ahsana, W.; Arshada, M. F.; *Acta. Chim. Slov.* **2009**, *56*, 462–469. http://acta-arhiv.chem-soc.si/56/56-2-462.pdf
51. Motati, D. R.; Amaradhi, R.; Ganesh, T.; Recent developments in the synthesis of azaindoles from pyridine and pyrrole building blocks. *Organic Chemistry Frontiers*, **2021**, *8*(3), 466-513. https://doi.org/10.1039/d0qo01079k
52. Sahiba, N.; Teli, P.; Agarwal, S.; "On Water" and "In Water" Strategies for Heterocyclic Transformations. *Advances in Organic Synthesis:* **2021**, *14*, 1. https://www.scribd.com/book/503036422/Advances-in-Organic-Synthesis-Volume-14
53. Phillips, A.M.M.F.; Pombeiro, A. J.; Microwave-assisted synthesis of fluoroorganics. *Green Sustainable Process for Chemical and Environmental Engineering and Science*, **2021**, 415-488. https://doi.org/10.1016/B978-0-12-819848-3.00010-4
54. Pagola, S.; Outstanding Advantages, Current Drawbacks, and Significant Recent Developments in Mechanochemistry: A Perspective View. *Crystals*, **2023**, *13*(1), 1-33. https://doi.org/10.3390/cryst13010124
55. Zhimomi, B.K.; Imchen, P.; Phucho, T.; Recent advances in strategies of green synthesis of 1, 3-oxazines-a brief review. *Tetrahedron*, **2022**, 132672. https://doi.org/10.1016/j.tet.2022.132672
56. Challa, C.S.; Katari, N.K.; Nallanchakravarthula, V.; Nayakanti, D.; Kapavarapu, R.; Pal, M.; Amberlyst-15 catalysed sonochemical synthesis of 2-amino-4, 6-disubstituted nicotinonitrile derivatives and their biological evaluation. *J. Mol. Strut*, **2021**, *1240*, 130541. https://doi.org/10.1016/j.molstruc.2021.130541
57. Mashweu, A.R.; Chhiba-Govindjee, V.P.; Bode, M.L.; Brady, D.; Substrate profiling of the cobalt nitrile hydratase from Rhodococcus rhodochrous ATCC BAA 870. *Molecules*, **2020**, *25*(1), 238. https://doi.org/10.3390/molecules25010238.
58. Bangale, S.; Jondhale, V.; Pansare, D.; Chavan, P.; Reusable ZnCr2O4 Nano Catalyzed One Pot Three-Component Cycloaddition Reaction for Synthesis of Azetidine Derivatives under Ultrasound Irradiation. *Poly. Aro. Comp*. **2021**, 6398-6410. https://doi.org/10.1080/10406638.2021.1983617
59. Chavan, P.; Salve, A.; Jadhav, S.; Pansare, D.; Rai, M.; Ultrasound assisted, synthesis of N-(7-(R)-2-oxa-8-azabicyclo[4.2.0]octan-8-yl)isonicotinamide derivatives and their biological evaluation. *J. Het. Chem.* **2020**, *57(3)*, 1228-1235. https://doi.org/10.1002/jhet.3860
60. Pansare, D. N.; Shelke, R. N.; Khade, M. C.; Jadhav, V. N.; Pawar, C. D.; Jadhav, R. A.; Bembalkar, S. R.; New thiazolone derivatives: design, synthesis, anticancer and antimicrobial activity. *Eur. Chem. Bull.* **2019**, *8(1)*, 7-14. https://doi.org/10.17628/ecb.2019.8.7-14
61. Pansare, D. N.; Shelke, R. N.; Pawar, C. D.; Sarkate, A. P.; Chavan, P. N.; Thopate, S. R.; Shinde, D. B.; Green synthesis of 4-methoxybenzylidene thiazole derivatives using potassium carbonate as base under ultrasound irradiation. *Curr. Chem. Lett.* **2019**, *8*, 1-14. https://doi.org/10.5267/j.ccl.2019.6.001
62. Chavan, P. N.; Pansare, D. N.; Shelke, R. N.; Eco-friendly, ultrasound-assisted, and facile synthesis of one-pot multicomponent reaction of acridine-1,8(2H,5H)-diones in an aqueous solvent. *J. Chin. Chem. Soc*. **2019**, 822-828. https://doi.org/10.1002/jccs.201800411
63. Chavan, P. N.; Pansare, D. N.; Jadhav, S. L.; Rai, M. J.; Synthesis and biological activities of new tetrahydroquinoline and pyrimidine derivatives. *Eur. Chem. Bull.* **2019**, *8(8)*, 257-264. https://doi.org/10.17628/ecb.2019.8.257-264
64. Kazi, S.; Nirwan, S.; Kunde, S.; Jadhav, S.; Rai, M.; Kamble, D.; Sayyed, S.; Chavan, P.; Green Synthesis, Characterization and Bio-evaluation of Zirconium Nanoparticles Using the Dried Biomass of Sphagneticola trilobata Plant Leaf. *BioNanoSci.* **2022**, *12*, 731–740. https://doi.org/10.1007/s12668-022-01006-9
65. Jadhav, S.; Farooqui, M.; Chavan, P.; Hussain, S.; Rai. M.; $ZnFe_2O_4$ Nano-Catalyzed One-Pot Multicomponent Synthesis of Substituted Tetrahydropyranoquinoline under Neat Ultrasonic Irradiation. *Poly. Aro. Com.*, **2020**, *42(5)*, 2067-2075. https://doi.org/10.1080/10406638.2020.1825005
66. Omar (Al-Ahdal), Z. T.; Jadhav, S.; Shejul, S.; Chavan, P.; Pathrikar, R.; Rai. M.; Synthesis, Magnetic Moment, Antibacterial, and Antifungal Studies of INH Incorporating Schiff Base Metal Complexes. *Pol. Aro. Comp.* **2022**, https://doi.org/10.1080/10406638.2022.2077776
67. Sonawane, H. R.; Deore, J. V.; Chavan, P. N.; Reusable Nano Catalysed Synthesis of Heterocycles: An Overview. *Chemistry Select*, **2020**, *7(8)*, https://doi.org/10.1002/slct.202103900

68. Wiegand, I.; Hilpert, K.; Hancock, R. E. W.; Agar and broth dilution methods to determine the minimal inhibitory concentration (MIC) of antimicrobial substances. *Nat. Protoc.* **2008**, *3*, 163–175. https://doi.org/10.1038/nprot.2007.521
69. Patterson, A.; The Scherrer Formula for X-Ray Particle Size Determination. *Phys. Rev.***1939**, *56*, 978–982. https://doi.org/10.1103/PhysRev.56.978
70. Singh, A.; Gautam, P. K.; Verma, A.; Singh, V.; Green synthesis of metallic nanoparticles as effective alternatives to treat antibiotics resistant bacterial infections: A review. *Biotechnol Reports* **2020**, *25*, e00427. https://doi.org/10.1016/j.btre.2020.e00427
71. Khalil, M. M. H.; Ismail, E. H.; El-Baghdady, K. Z.; Mohamed, D.; Green synthesis of silver nanoparticles using olive leaf extract and its antibacterial activity. *Arab. J. Chem.* **2014**,*7*, 1131–1139. https://doi.org/10.1016/j.arabjc.2013.04.007
72. Franci, G.; Falanga, A.; Galdiero, S.; Palomba, L.; Rai, M.; G. Morelli, M. Galdiero, Silver Nanoparticles as Potential Antibacterial Agents. *Molecules*. **2015**, *20*, 8856–8874. https://doi.org/10.3390/molecules20058856

Supplementary materials

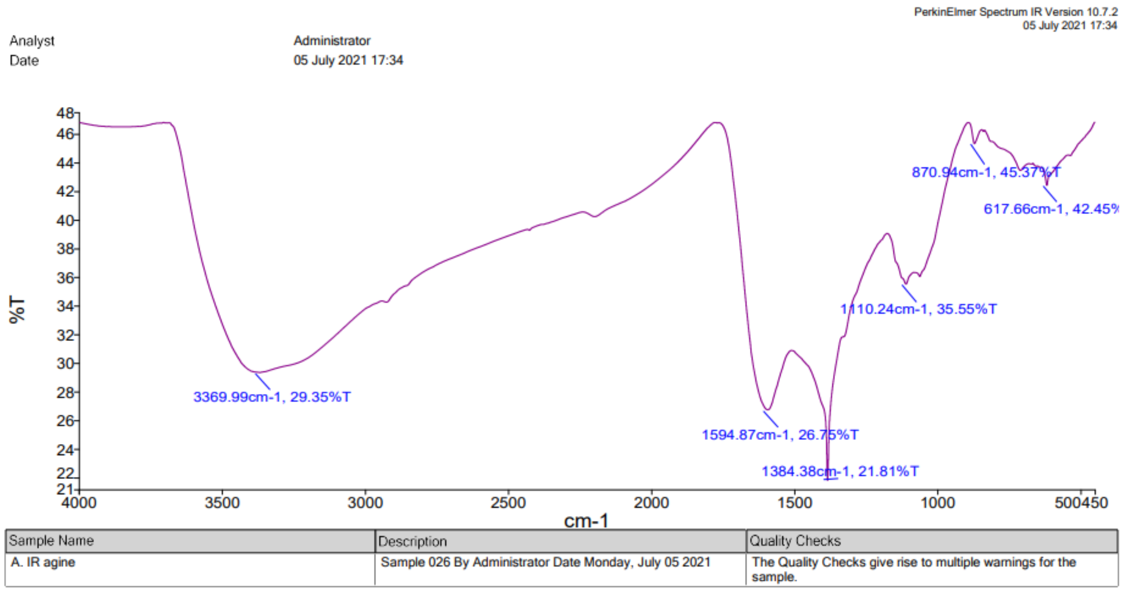

Figure S1. AgNPs FTIR.

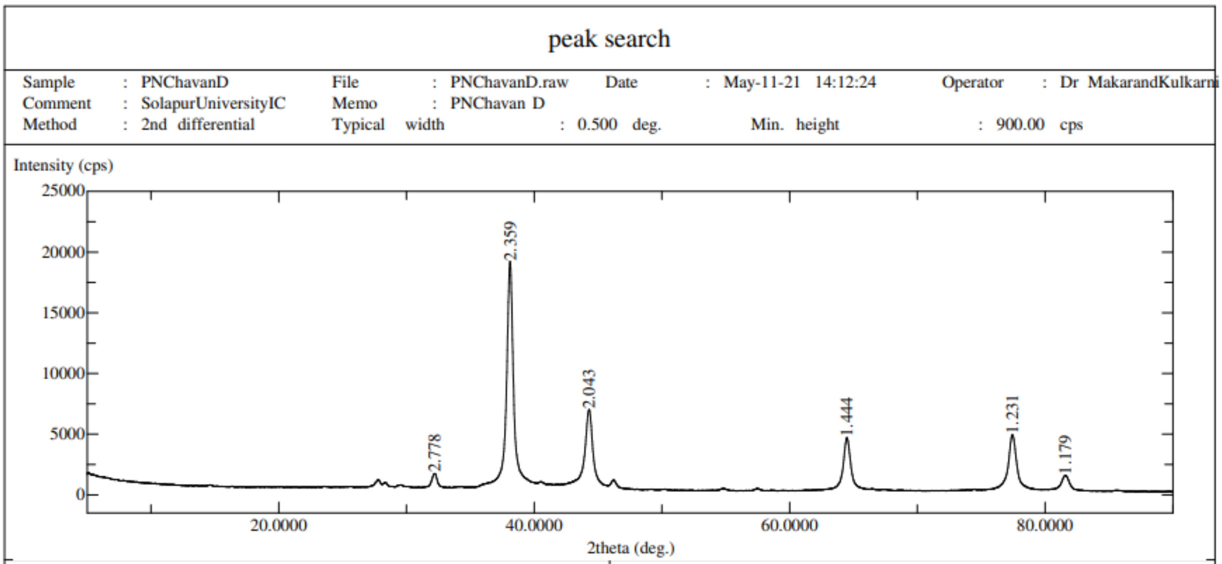

Peak no.	2theta	Flex Width	d-value	Intensity	I/Io
1	32.200	0.471	2.7776	1740	10
2	38.120	0.471	2.3588	19206	100
3	44.300	0.518	2.0430	7010	37
4	64.480	0.518	1.4439	4708	25
5	77.440	0.565	1.2314	4937	26
6	81.580	0.635	1.1791	1607	9

Figure S2. XRD-AgNPs.

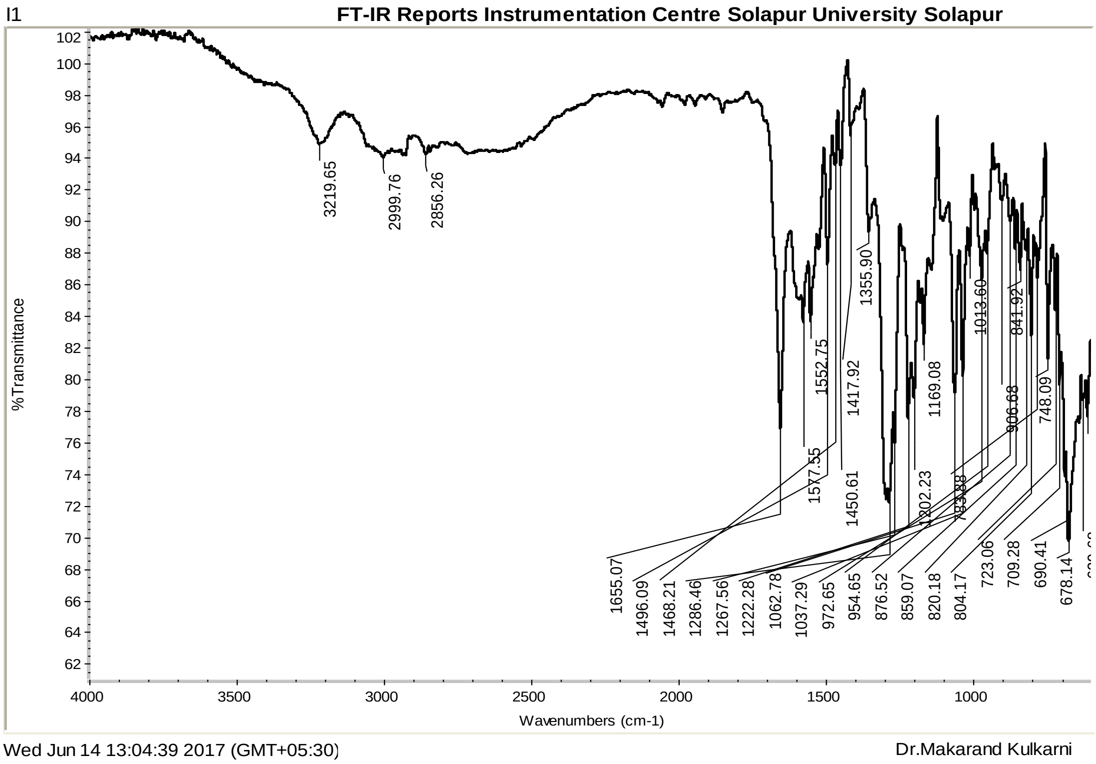

Figure S3. COMPOUND NO. (4c) 2,5-dimethoxybenzaldehyde.

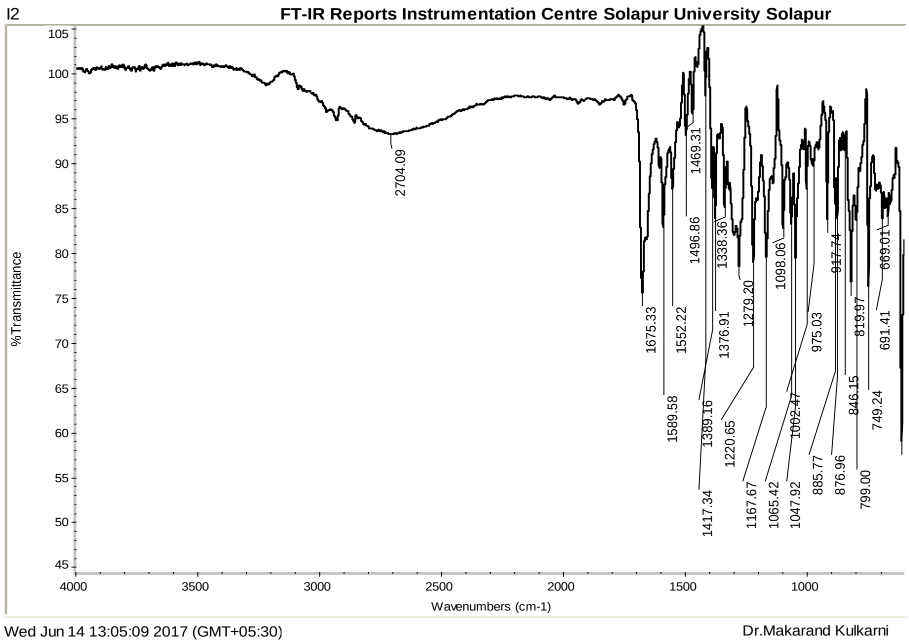

Figure S4. Compound No. (4h) 3,4-dihydroxybenzaldehyde.

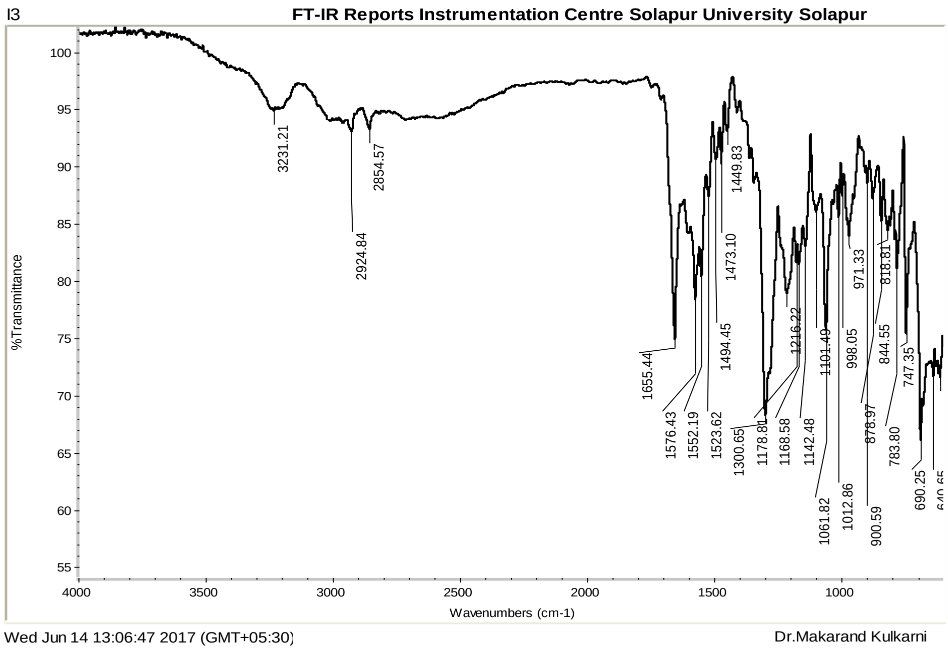

Figure S5. Compound No. (4d) 3-hydroxybenzaldehyde.

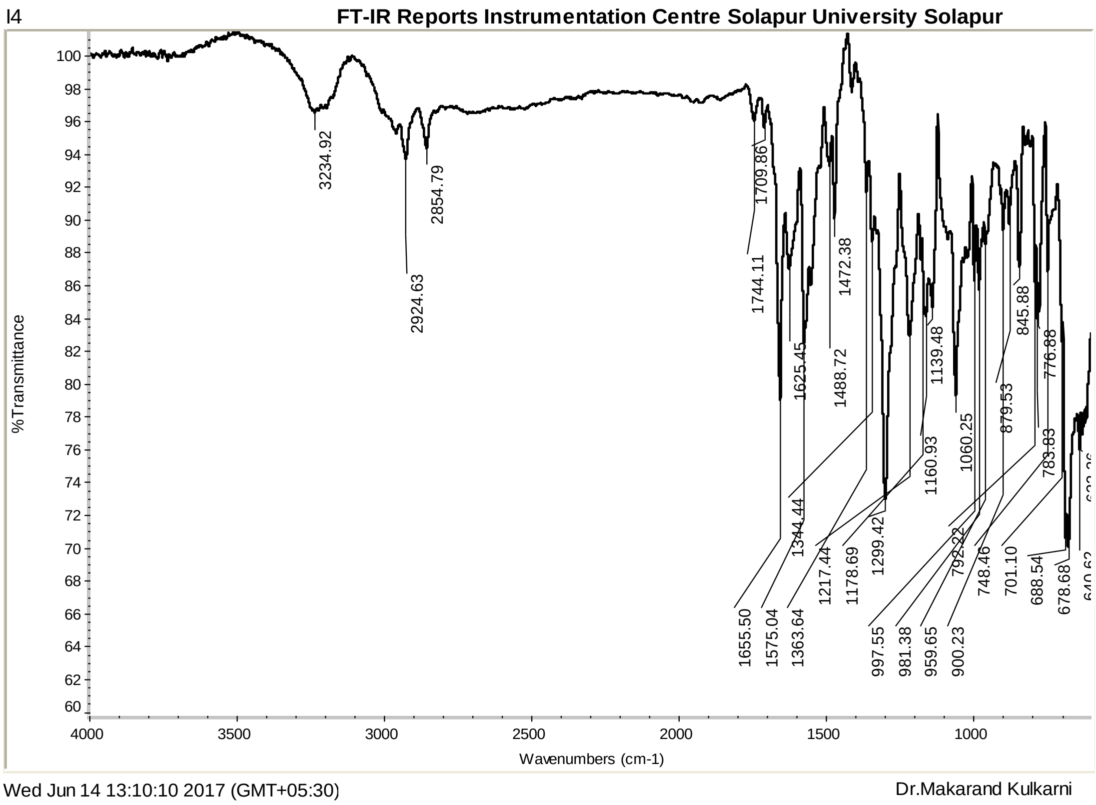

Figure S6. Compound No. (4b) 4-cynobenzaldehyde.

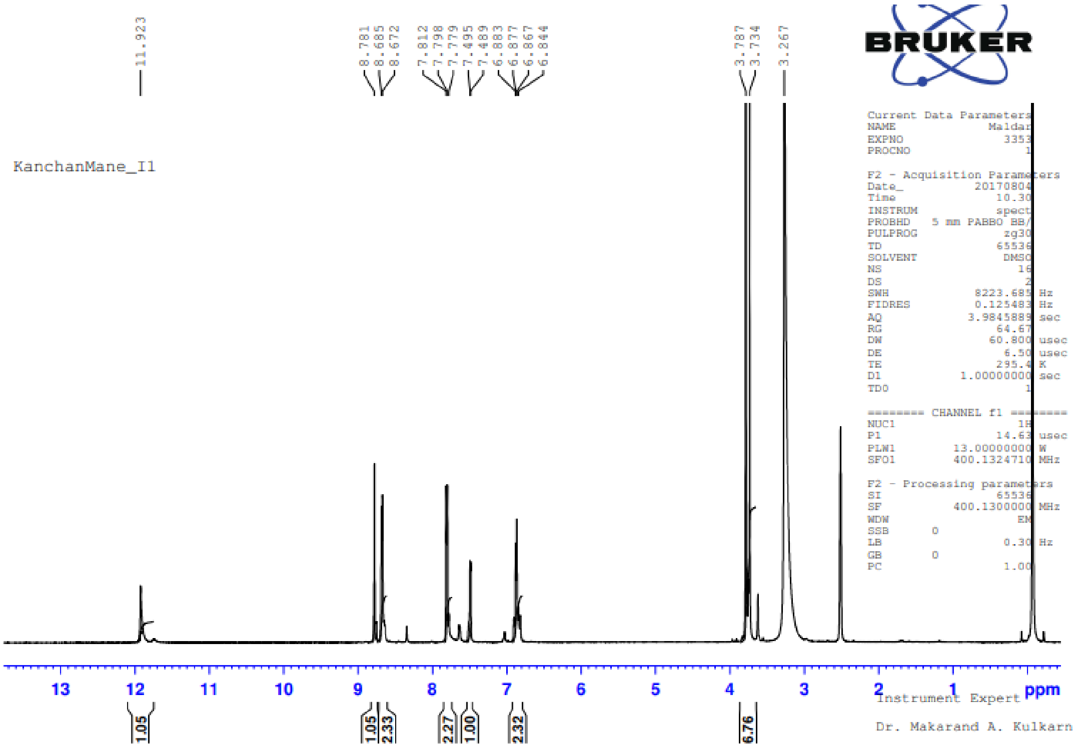

Figure S7. [1]H NMR Compound No. (4c) 2,5-dimethoxybenzaldehyde.

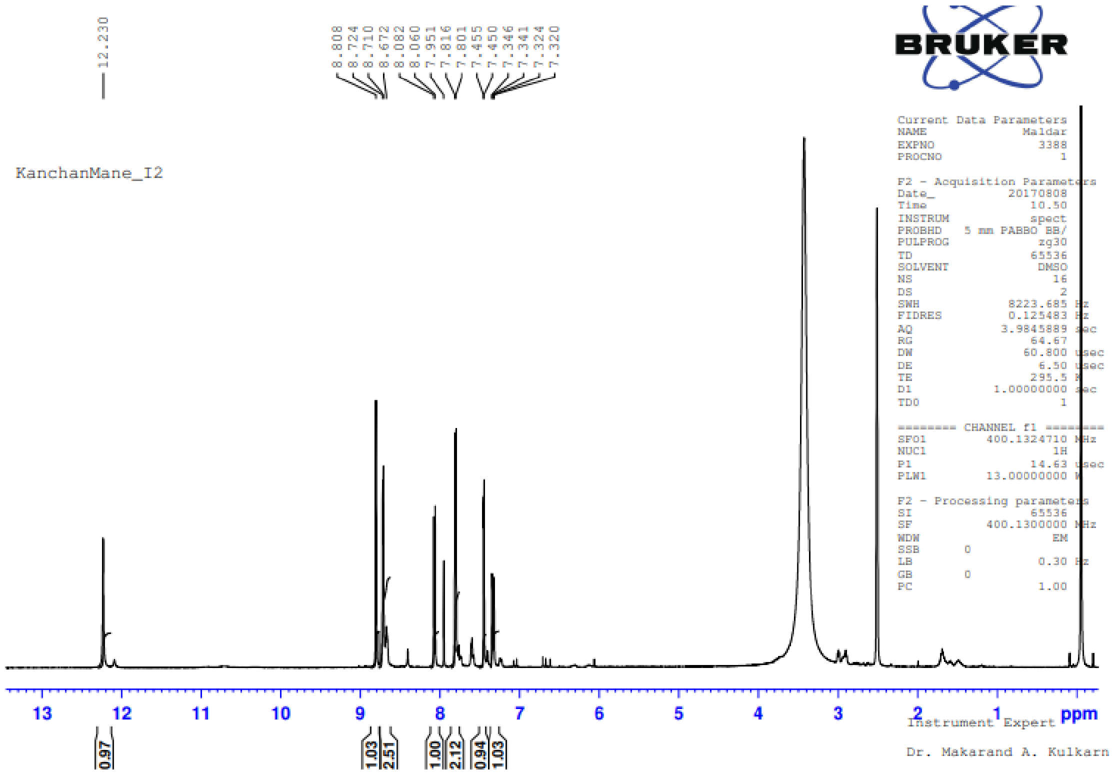

Figure S8. Compound No. (4h) 3,4-dihydroxybenzaldehyde.

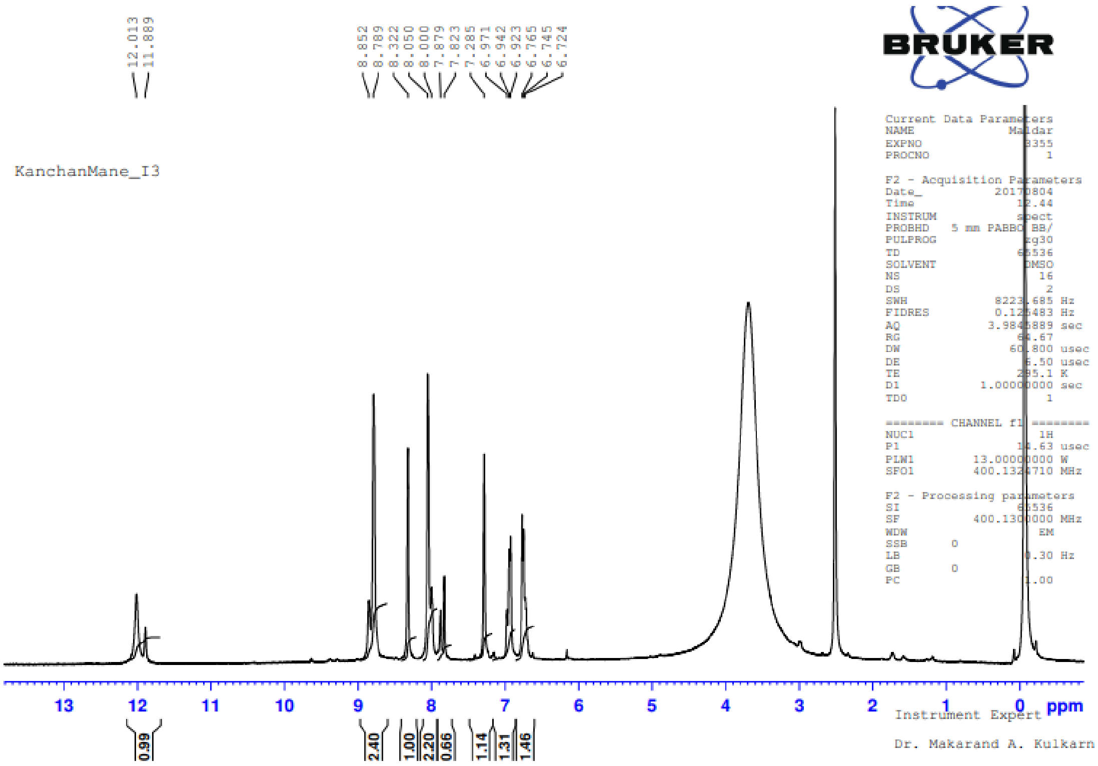

Figure S9. Compound No. (4d) 3-hydroxybenzaldehyde.

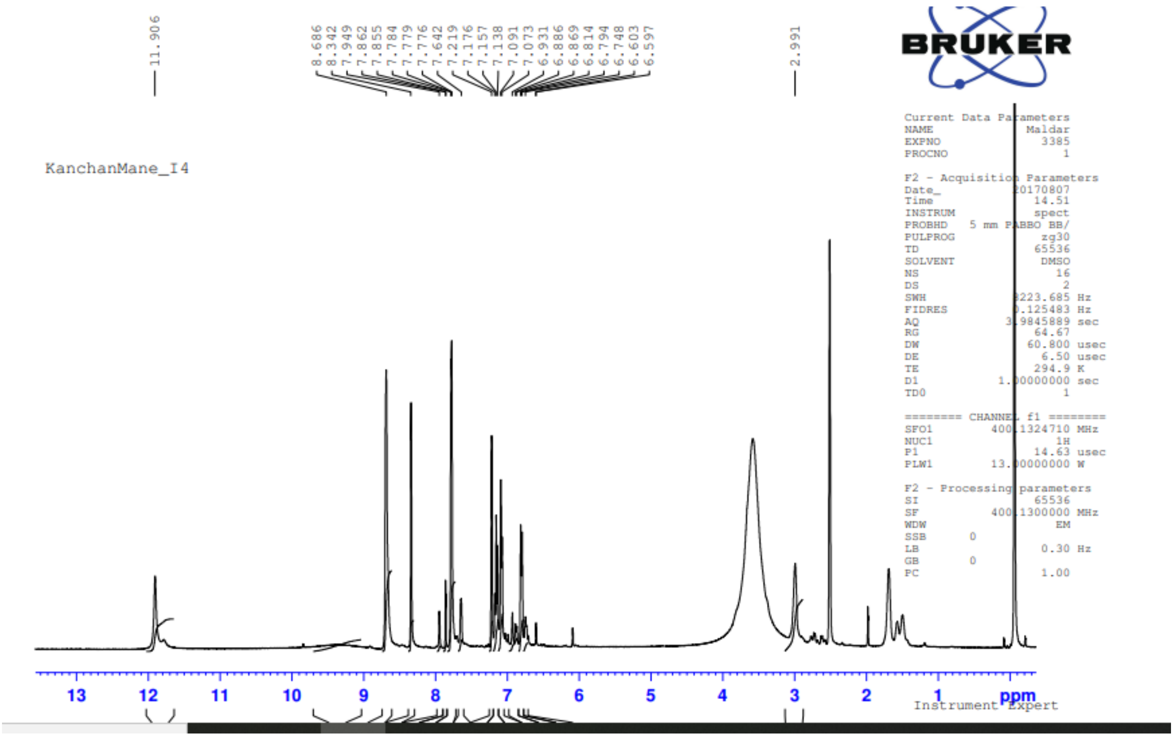

Figure S10. Compound No. (4b) 4-cynobenzaldehyde.

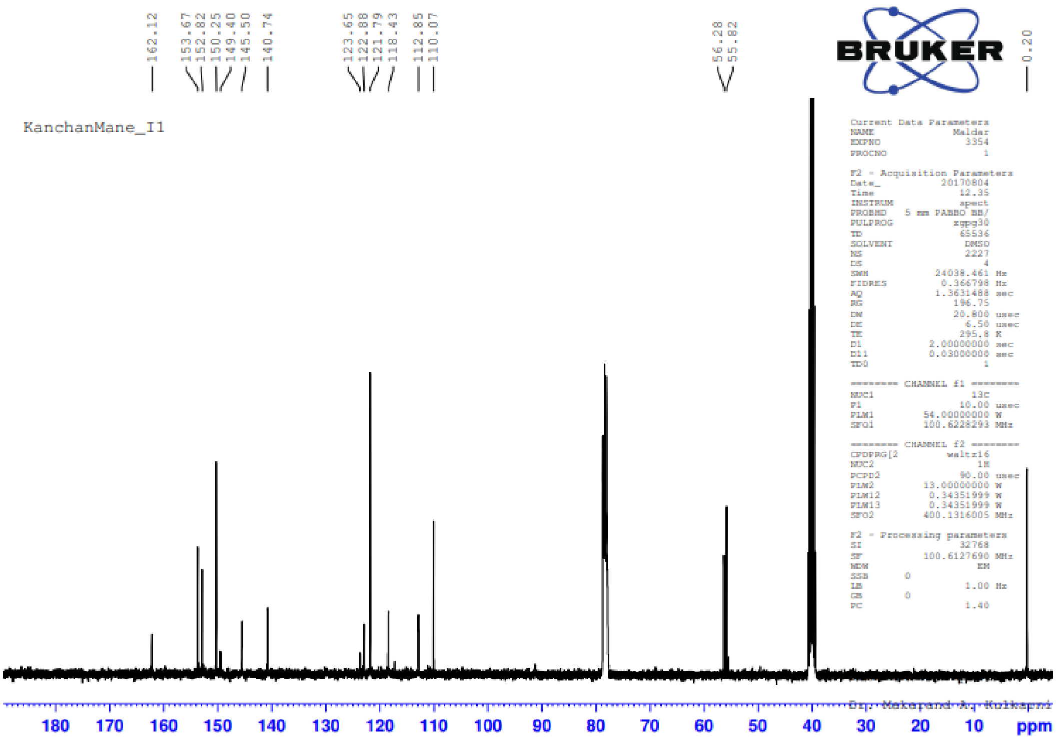

Figure S11. [13]C NMR of compound no. (4c) 2,5-dimethoxybenzaldehyde.

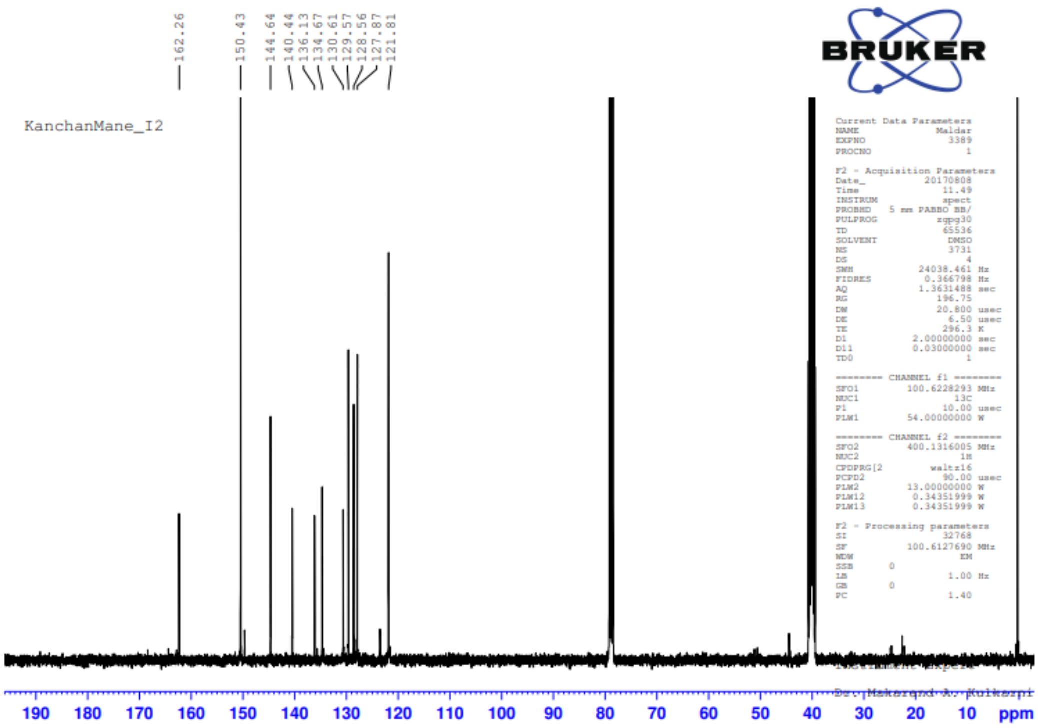

Figure S12. Compound no. (4h) 3,4-dihydroxybenzaldehyde.

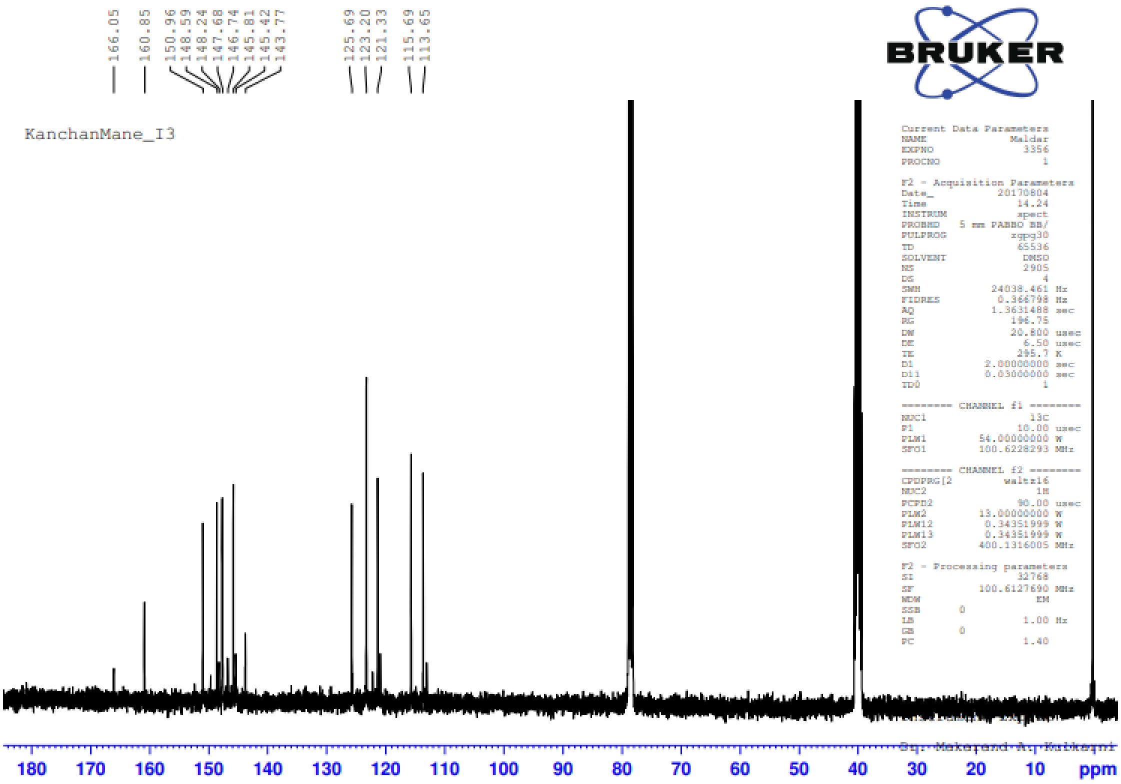

Figure S13. Compound no. (4d) 3-hydroxybenzaldehyde.

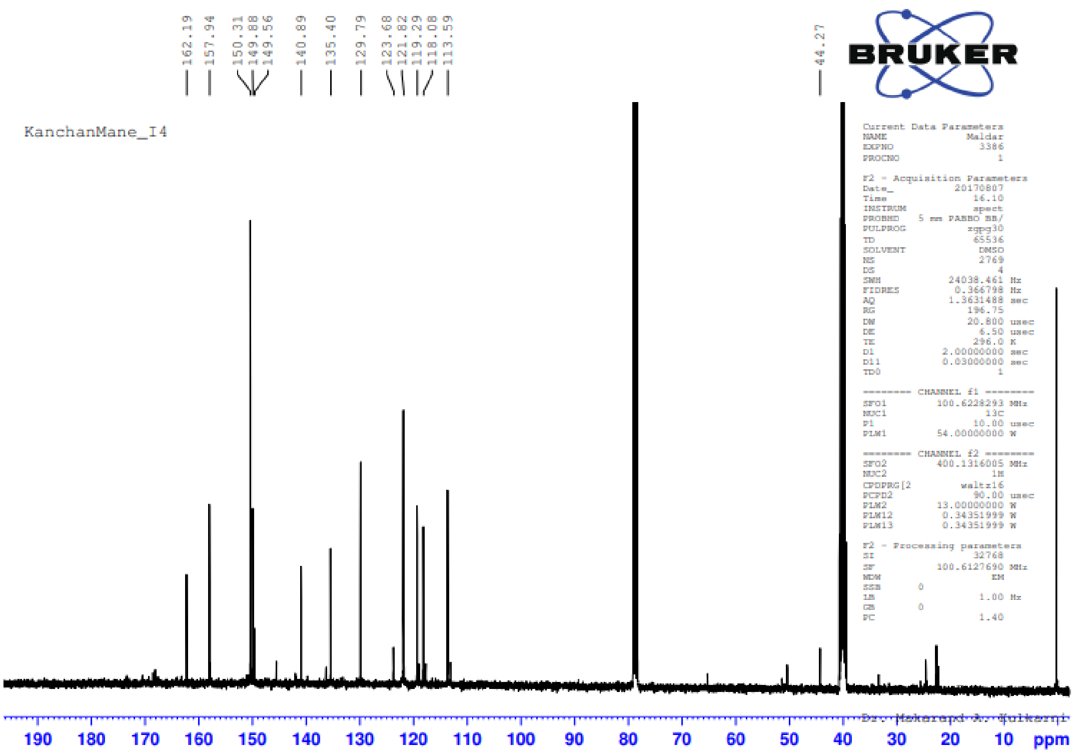

Figure S14. Compound no. (4b) 4-cynobenzaldehyde.